Solvent and Ligand Effects on the Localized Surface Plasmon Resonance (LSPR) of Gold Colloids

Sujit Kumar Ghosh, Sudip Nath, Subrata Kundu, Kunio Esumi,† and Tarasankar Pal*

Department of Chemistry, Indian Institute of Technology, Kharagpur-721302, India, and Department of Applied Chemistry, Tokyo University of Science, Tokyo-162-8601, Japan

Received: July 6, 2004

Cetylpyridinium chloride(CPC)-stabilized gold organosol in toluene has been prepared by using a two-phase (water−toluene) extraction of $AuCl_4^-$ followed by its reduction with sodium borohydride in the presence of the surfactant, CPC. The surfactant-stabilized gold nanoparticles were exploited to examine their optical properties when exposed to various solvent systems and ligands by measuring the changes in the localized surface plasmon resonance (LSPR) spectrum. It was seen that the position of the surface plasmon band of metal nanoparticles is greatly influenced by the solvents and the ligands under consideration. The surface plasmon absorption maxima modulates/varies between 520 and 550 nm for gold nanoparticles, depending on the refractive index of the solvent. The significant discovery presented here is that λ_{max} of the LSPR shifts to the blue by 3 nm for the increase of one carbon atom in the alcohol chain. Cationic and anionic surfactants of different chain lengths induce changes in the optical properties of gold nanoparticles, whereas zwitterionic amino acid molecules do not incite remarkable changes in the LSPR spectrum. The λ_{max} of the LSPR gradually shifts to the red with the increase in chain length for both the cationic and anionic surfactants indicating specific binding of the surfactant molecules around the gold particles. Binding of three model compounds (1-dodecylamine, 1-dodecanol, and 1-dodecanethiol) indicates their relative affinity toward the gold surface that corroborate the HSAB (Hard−Soft Acid−Base) principle.

1. Introduction

In recent years, organosols of gold and other noble metals have attracted considerable interest from researchers as the solvents leave their direct impression on the electronic and optical properties of the sol system.[1−6] Functional groups such as thiols, amines, or silanes have commonly been used to prepare stable gold nanoparticles in aqueous media. Efforts to apply this chemical-functionalization concept to prepare metal nanoparticles in organic solvents have often encountered stability problems. Again, without the application of organosol systems the study often fails to register the impacts of the solvent on the sol properties. Therefore, preparation of stable metallic particles with sizes in the nanometer regime requires a great deal of control over the synthetic technique. Different synthetic strategies have been adopted for the preparation of metal particles in organic solvents and different capping agents have been used to stabilize them.[7−15] Brust et al.[7] reported the synthesis of dodecanethiol-derivatized gold nanoparticles in a two-phase liquid−liquid system. Rao et al.[9] described the synthesis of thiol-derivatized nanoparticles of Au, Ag, and Pt by the acid-induced transfer of hydrosol to a toluene layer containing thiol. Nakao[10] reported the conversion of a gold hydrosol stabilized by cetylpyridinium chloride (CPC), to a gold organosol in chloroform and its subsequent discoloration by photoirradiation. Stable colloids of Pd, Pt, and Au have also been prepared in polar solvents such as acetone, ethanol, 2-propanol, DMF, DMSO, or THF.[11] Esumi et al.[12] described the preparation of dendrimer-encapsulated gold nanoparticles by the reduction of $HAuCl_4$ with $NaBH_4$ in formamide or *N*,*N*-dimethylformamide, and so on.

The optical properties of noble metal nanoclusters have fascinated scientists since the recent past because of their applications as functional materials in optical devices,[16,17] optical energy transport,[18,19] near-field scanning optical microscopy (NSOM),[20−23] surface enhanced Raman scattering spectroscopy,[24−29] and chemical and biological sensors.[30−35] Characteristically, noble metal nanoparticles exhibit a strong absorption band in the visible region and this is indeed a small particle effect, since they are absent in the individual atom as well as in the bulk.[36,37] The physical origin of the light absorption by metal nanoparticles is the coherent oscillation of the conduction band electrons induced by the interacting electromagnetic field. The absorption band results when the incident photon frequency is resonant with the collective oscillation of the conduction band electrons and is known as the localized surface plasmon resonance (LSPR). The resonance frequency of this LSPR is strongly dependent upon the size, shape, dielectric properties, and local environment of the nanoparticle.[36,38−42] The oscillation frequency is critically determined by four factors: the density of electrons, the effective electron mass, and the shape and size of the charge distribution. Moreover, for a metal such as gold, the plasmon frequency is also influenced by the d-orbital electrons. Real-time monitoring of the optical properties of a system of metallic nanoparticles requires taking the following parameters into consideration: the presence of a supporting substrate and/or stabilizing ligand shell, a solvent layer on the top of the particles, and electromagnetic interactions between the particles that are close enough in the ensemble to influence the optical properties.[43−46]

The optical properties of gold sols have attracted attention ever since the Romans began to use them for brilliant red staining in glass windows. These properties of noble-metal sols

* E-mail: tpal@chem.iitkgp.ernet.in.
† Tokyo University of Science.

10.1021/jp047021q CCC: $27.50
Published on Web 08/24/2004

have been of interest for centuries, but scientific research on metal particles was initiated by Michael Faraday[47] and it was one of the great triumphs of classical physics when, in 1908, Mie presented a solution by solving Maxwell's equations[48−50] to explain the color of the gold sol. The interesting colors observed in gold sols have led to extensive study of their optical spectroscopic properties in an effort to correlate their behavior under different microenvironmental conditions. Most of the recent reports adopt a variation of the method reported by Brust et al.,[7] which involves a two-phase (water−toluene) extraction, followed by the reduction of $[AuCl_4]^-$ in the presence of alkanethiol. These studies focus on the synthesis of thiol-capped gold nanoparticles, and little effort has been made to understand the mode of interaction of the metal particle surface with the binding agents and solvent molecules. Thiol-capped nanoparticles exhibit strong interaction between the metal surface and the organic binding agent as evident from the complete dampening of the surface plasmon band. The loss of plasmon absorption in such systems limits the spectroscopic investigations on the influence of the solvent environment on the surface of the metal nanoparticle.

In this article, we describe a straightforward procedure to obtain cetylpyridinium chloride (CPC)−stabilized gold nanoparticles in a nonpolar solvent (toluene). The particles were characterized by UV−visible spectroscopy and transmission electron microscopic (TEM) studies. The CPC-stabilized gold nanoparticles were exploited to study their optical properties when exposed to various solvents and binding agents by measuring the changes in the localized surface plasmon resonance (LSPR) spectrum of the metal particles. This approach is a simplified dictation of the LSPR studies as an alternative to the nanosphere lithography (NSL) technique. It is seen that the position of the surface plasmon band of metal nanoparticles is greatly influenced by the solvent and binding agents under consideration. The surface plasmon peak position interplays between 520 and 550 nm for gold nanoparticles, depending on the refractive index of the chosen solvent. In the present study, the electromagnetic interactions between the gold particles do not come into play as the metal particles are sufficiently dispersed and may be treated as being isolated. We have made a detailed investigation of the LSPR of gold nanoparticles when exposed to a series of alcohols of variable chain length, $CH_3(CH_2)_{x-1}OH$, where, $x = 1-10$. The λ_{max} of the LSPR shifts to blue by 3 nm for the addition of every carbon atom to the alcohol chain. Again, the surfactant-induced changes in the LSPR were detected by employing a series of cationic and anionic surfactants of different chain lengths to cationic surfactant-stabilized gold nanoparticles. The λ_{max} of the LSPR gradually shifts to the red with the increase in chain length of both of the cationic and anionic surfactant. whereas no detectable changes were observed when zwitterionic amino acids were employed in lieu of surfactants. Binding studies with three model compounds (1-dodecylamine, 1-dodecanol, and 1-dodecanethiol) indicates their preferential affinity to the gold surface in accordance to HSAB principle.

2. Experimental Section

2.1. Reagents and Instruments. All of the reagents were of AR grade and all of the solvents were dried. Chloroauric acid ($HAuCl_4 . xH_2O$), cetylpyridinium chloride, sodium borohydride, and toluene were purchased from Aldrich. Cetyltrimethylammonium chloride (C_{16}TAC) and other cationic surfactants of different chain length (C_{10}, C_{12}, and C_{14}) of the same homologous series were obtained from Aldrich and were used without further purification. Anionic surfactants, sodium dodecyl sulfate (SDS), decylsodium sulfate (DSS), and sodium dodecyl benzene sulfonate (SDBS) were purchased from Sigma and were used as received. The reagents 1-dodecylamine (DDA), 1-dodecanol (DDO), and 1-dodecanethiol (DDT) were purchased from Aldrich and were used without purification.

The absorption spectrum of each solution was recorded in a Spectrascan UV 2600 digital spectrophotometer (Chemito, India) in a 1-cm well-stoppered quartz cuvette and the solvent background was subtracted each time. Electron micrographs of the metal colloids were taken with a Hitachi H-9000NAR transmission electron microscope, operating at 200 kV. The samples were prepared by mounting a drop of the solution on a carbon-coated copper grid and allowing it to dry in air.

2.2. Preparation of Gold Nanoparticles in Toluene. The preparation of the CPC-stabilized gold nanoparticles was carried out in a single-phase system. In a typical preparation, $AuCl_4^-$ was first transferred from an aqueous solution to toluene using tetraethylammonium chloride as the phase transfer reagent and was then reduced with sodium borohydride in the presence of a cationic surfactant, CPC as the stabilizing agent. Upon addition of the reducing agent, the toluenic solution changed color from light yellow to wine red within a few minutes.

The preparation technique is as follows. To an aqueous solution of chloroauric acid (5 mL, 2.0 mM), 20 mg of tetraethylammonium chloride was added and toluene was introduced above the aqueous layer. The addition of the phase transfer reagent to the aqueous phase caused swift movement of the $AuCl_4^-$ ions to the organic layer. The total amount of $AuCl_4^-$ ions was extracted with 20 mL of toluene (preferably in 3−4 successive stages to facilitate the quantitative transfer of the interface). To this solution was added 10 mg of CPC and the solution was mixed well. Finally, 2 mg of sodium borohydride was introduced and the reaction mixture was shaken vigorously. During shaking, at first, the yellow color of $AuCl_4^-$ was found to disappear and the solution became colorless after ~8 min. Then, the solution slowly turned to red and became wine red after ~12 min. This indicated the formation of gold nanoparticles. After the solution became wine red, the sol showed no further change in color, implying the completion of the reaction. The method is reproducible and the organosol prepared by this method remains stable after a couple of months even if stored at room temperature. The final concentration of gold in this experiment was 0.5 mM. The metallic particles dispersed in toluene can be dried under vacuum and redispersed well in common organic solvents without any sign of aggregation or precipitation of the particles.

3. Results and Discussion

3.1. Evolution of Gold Nanoparticles in Toluene. Figure 1 shows the absorption spectral features for the evolution of gold nanoparticles in toluene. The toluenic dispersion of the cationic surfactant, cetylpyridinium chloride, shows no characteristic absorption maximum in the range of 300−700 nm (trace a). The $AuCl_4^-$ ions in toluene exhibit an absorption peak at 323 nm (trace b) that can be attributed to the metal-to-ligand charge transfer (MLCT) band of $AuCl_4^-$ complexes.[51] Addition of CPC to the toluenic solution of Au(III) causes the 323-nm absorption band to vanish due to $AuCl_4^-$ complexes. A new absorption band appears with a shoulder at ~ 355 nm (trace c) that can be ascribed to the formation of an ion pair $[CP]^+[AuCl_4]^-$, ($[CP]^+$ = cetylpyridinium ion).[51] Upon addition of $NaBH_4$ to the reaction mixture, the yellow color of the solution gradually disappears and after a certain time, the solution becomes

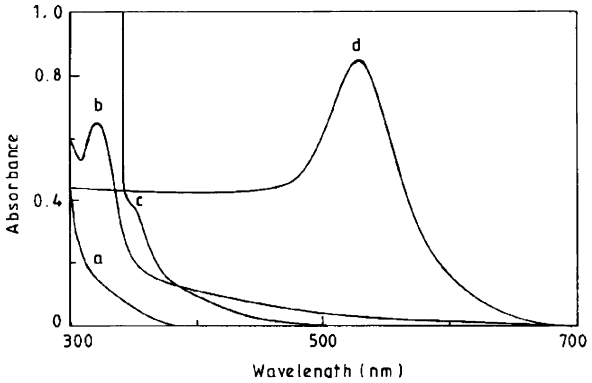

Figure 1. Absorption spectrum of (a) CPC dispersed in toluene, (b) $HAuCl_4$ in toluene, (c) after addition of CPC to $HAuCl_4$ in toluene, and (d) gold nanoparticles in toluene. Condition: $[HAuCl_4] = 0.5$ mM, Amount of CPC = 10 mg. The volume of the solution was 20 mL with toluene.

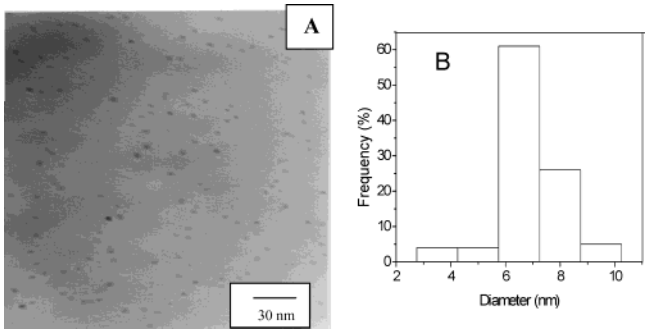

Figure 2. (A) TEM images and (B) diameter histogram of the CPC-stabilized gold organosol.

completely colorless indicating the formation of AuO_2^- species in the alkaline condition.[52] On further shaking, the appearance of the pinkish tinge within the solution indicates the onset of the evolution of the gold particles. The color of the solution gradually changes from light pink to red to wine red upon completion of the reaction. Absorption measurement of this resulting solution shows a new absorption band with a maximum at 530 nm (trace d), which corresponds to a typical plasmon band of gold nanoparticles. Transmission electron micrographs (Figure 2) of the gold particles show that the particles are nearly spherical with a mean diameter of 6 ± 0.2 nm.

3.2. Effect of Solvent on the LSPR of Gold Colloids. *3.2.1. Effect of Solvent Refractive Index and Functionality.* Many research activities have been put forward in the literature concerning the effect of solvent refractive index on the optical properties of metal nanoparticles prepared under different synthetic conditions. These investigations provide distinct information in accounting for the effect of solvent refractive index. For example, Papavassiliou[53] observed that the color of the noble metal sols of Cu, Ag, and Au are quite sensitive to the change in the refractive index of the solvent medium. In contrast to this observation, Hostetler et al.[54] observed that spectra of modestly dispersed monolayer-protected clusters (MPCs) of gold (4.4 nm average diameter) in solvents of various refractive indices displayed distinct surface plasmon bands that did not noticeably shift in energy. Recent studies have shown that the effect of the solvent refractive index on the color of the polymer-stabilized gold sol was in agreement with the Mie theory.[55] In their investigation of the effect of surface plasmon absorption of gold nanoparticles, stabilized with a *comb* polymer, Underwood and Mulvaney[55] observed a 10-nm shift in the surface plasmon absorption of gold nanoparticles when

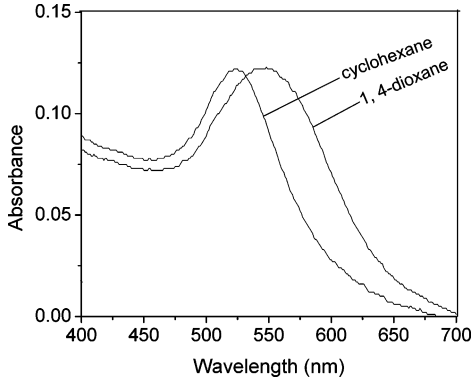

Figure 3. Localized surface plasmon resonance (LSPR) of gold nanoparticles (50 μM) in cyclohexane and 1, 4-dioxane.

the solvent refractive index was varied from $n_d^{20} = 1.375$ (hexane) to $n_d^{20} = 1.5010$ (benzene). In another study, Murray et al.[4] noted that the solution spectra of dodecanethiolate MPCs (5.2 nm average diameter) reveal an 8-nm shift in plasmon band position as the solvent refractive index is varied from $n_d^{20} = 1.33$ to 1.55. The spectral shifts agree well with the predictions of Mie theory when the alkanethiolate monolayer is accounted for in the calculation. Recently, Malinsky et al.[1] explored the optical properties of silver nanoparticles which were fabricated using the technique of nanosphere lithography and reported that unmodified Ag particles undergo structural changes when exposed to various solvents that significantly affect the LSPR.

We have studied the optical properties of the surfactant-stabilized (i.e., CPC-stabilized) gold nanoparticles when they are exposed to various solvents by measuring the LSPR spectrum of the metal particles. It is found that the absorption spectrum, λ_{max}, of the gold sol is extremely susceptible to the alteration of the refractive index of the solvent system. To study the solvent effect on metal colloids, the stability of the metallic nanoparticles in the solution phase is an important issue as naked metal nanoparticles are unstable in organic solvents. Moreover, the comparison of the spectra very often becomes fortuitous due to differences in particle shape, size distribution, impurity absorption, and coalescence between the particles. Such phenomena create a major problem for investigating the dependence of surface plasmon absorption on the refractive index of the medium. Therefore, to establish a correlation, it is desirable to use nanoparticles with tight size distribution and stabilized by a capping agent with the same type of functional group. The present method offers CPC-stabilized gold nanoparticles in toluene with a narrow size distribution. The CPC-stabilized gold nanoparticles can be transferred to a variety of organic solvent systems without any aggregation.

To gain a clear insight into the dependence of the surface plasmon band position of gold sol on the refractive index, the gold suspension in toluene was suspended in a sequence of polar and nonpolar solvents. In practice, the organosol prepared by the above method was evaporated to ca. 2 mL in a rotary evaporator, resulting into a gold concentration of 5.0 mM. An aliquot of 20 μL of this highly concentrated gold suspension was diluted to 2 mL with the desired solvents (all the solutions thus contained $\sim$1% of toluene, the final concentration of gold was 50 μM), and the normalized LSPR spectra of all the solutions were measured. Figure 3 shows the response of the LSPR of gold nanoparticles to the changes in medium dielectric constant in cyclohexane and 1, 4-dioxane, respectively. The LSPR suffered a red shift of $\sim$23 nm when the solvent was substituted with 1,4-dioxane in place of cyclohexane. The position of the surface plasmon band maximum, λ_{max} with the

TABLE 1: Absorption Maxima of LSPR of CPC-Stabilized Gold Nanoparticles in Solvents of Varying Refractive Indices

solvent	refractive index (n)	λ_{max} (nm)
cyclohexane	1.4262	519.5
chloroform	1.4486	521.5
carbon tetrachloride	1.4600	526
toluene	1.4969	530
o-xylene	1.5054	532
acetonitrile	1.3441	545.5
tetrahydrofuran	1.4072	526
1, 4-dioxane	1.4224	542.5
dimethylformamide	1.4282	549
dimethyl sulfoxide	1.4790	542

variation in solvent refractive indices, is illustrated in Table 1. A close inspection of the results in Table 1 shows that the interaction of the solvents with the gold particles follows two different trends. In some cases, the variation of the λ_{max} of the LSPR is linearly dependent on the refractive index of the solvent (n) whereas, in some other cases, a nonlinear variation is observed. This can be accounted for as follows. Solvents (cyclohexane, chloroform, carbon tetrachloride, toluene, and *o*-xylene) do not possess any active functional groups and remain inert, with no noticeable chemical interactions with the gold surfaces. The λ_{max} of the LSPR of gold nanoparticles in these solvents gradually shifts toward red with the increase in solvent refractive index. On the other hand, solvents such as acetonitrile (CH_3CN), tetrahydrofuran (THF), 1,4-dioxane, dimethylformamide (DMF), and dimethyl sulfoxide (DMSO) show the nonlinear dependence of the absorption maximum of the gold colloid with the solvent refractive index. These polar solvents are capable of complexing with gold surfaces through direct charge−transfer interaction and they have different extents of electron injection capabilities. Gold atoms at the surface of the particles are coordinatively unsaturated, that is, unoccupied orbitals are available for the nucleophiles to donate electron density. As a result, small metallic particles of gold have a high electron affinity and can strip electrons from such solvent molecules.[56] In accordance to Mie theory,[48] the addition or removal of electrons from colloidal particles produces a notable shift in the plasmon band position.[57,58] In the present case, the amount of available electrons from different solvent molecules differs and that is responsible for the variation in LSPR of the gold particles in these polar solvent systems. The resulting charged particles are stabilized by the solvent molecules, and the repulsive force between the charged particles prevents their aggregation.[59−61] These results are in contrast to the earlier observation of George Thomas et al.,[5] as a large TOAB shell engenders bulk solvent molecules' penetration and affects the interaction with the gold surfaces.

The linear variation of the maxima of LSPR with the refractive index of the solvent can be treated within the framework of the Drude model. According to the Drude model, the surface plasmon peak position, λ, is related to the refractive index of the surrounding medium (n) by the relation[62]

$$\lambda^2 = \lambda_p{}^2 (\epsilon^\infty + 2\epsilon_m) \quad (1)$$

where λ_p is the bulk metal plasmon wavelength, ϵ^∞ is the high-frequency dielectric constant due to interband and core transitions, and ϵ_m ($= n^2$) is the optical dielectric function of the medium. From the eq 1, it is evident that from the plot of λ^2 vs $2\epsilon_m$ we can extract the information about the bulk plasmon frequency of the metal. Figure 4 shows a plot of the square of the observed position (λ^2) of the LSRP of gold nanoparticles in a sequence of solvents, as a function of twice the medium dielectric function. The linear variation of the λ_{max} of the LSPR with the medium dielectric function is indicative of the fact that the solvent refractive index influences the surface plasmon maximum according to the Drude model. Therefore, it can be inferred that although the surfactant molecules surrounding the nanoparticle acts as a barrier preventing solvent penetration to the surface, the electromagnetic fields of gold remain extended to sense refractive index changes occurring at the CPC/bulk interface.

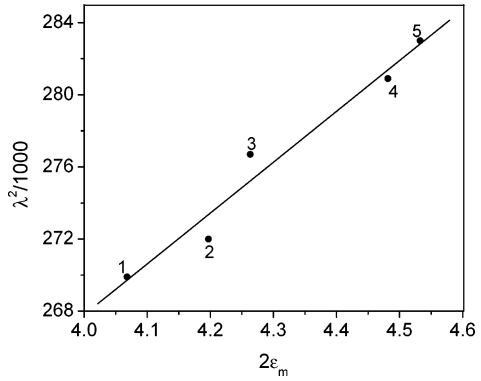

Figure 4. Plot of the square of the absorption maxima as a function of twice the medium dielectric function (ϵ_m was determined from the expression, $\epsilon_m = n^2$). Integers 1, 2, 3, 4, and 5 on the curve represent cyclohexane, chloroform, carbon tetrachloride, toluene, and *o*-xylene, respectively.

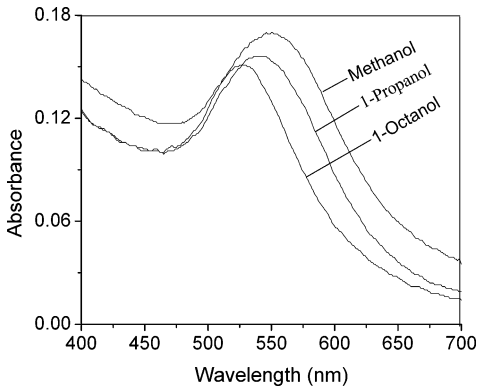

Figure 5. Surface plasmon absorption band of gold nanoparticles (50 μM) in methanol, 1-propanol, and 1-octanol.

3.2.2. Effect of Solvent Chain Length. The dependence of the LSPR spectrum of the gold nanoparticles was investigated as a function of the chain length of the alcohol. In this event, a series of alcohols with variable chain length, $CH_3(CH_2)_{x-1}OH$ where $x = 1-10$, was elegantly employed. An aliquot of 20 μL of highly concentrated gold suspension (5.0 mM) was diluted to 2 mL with the respective alcohol and absorption spectrum of each solution noted. It was seen that the chain length of the alcohol has a dramatic influence on the LSPR of the CPC-stabilized gold particles. Figure 5 illustrates the representative plasmon absorption band of the gold particles in methanol, 1-propanol, and 1-octanol, respectively. The maximum of plasmon absorption in methanol appears at 547 nm and successively shifts to the blue by 3 nm for the increase of every carbon atom in the alcohol chain. The dependence of the LSPR, λ_{max}, as a function of the number of carbon atoms on the alcohol chain is shown in Figure 6. Although the plasmon absorption band of gold nanoparticles is broad in nature in some cases, the absorption maxima are reported to show the trend. The most interesting feature of this investigation is that though the refractive index of the alcohols increases from methanol to decanol, the absorption maxima of the gold particles in these

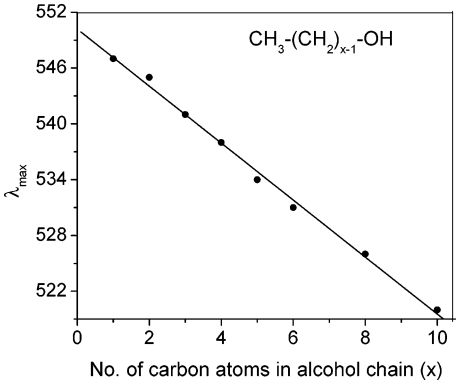

Figure 6. Dependence of the observed peak position of the LSPR spectra of gold nanoparticles on the chain length of alcohol.

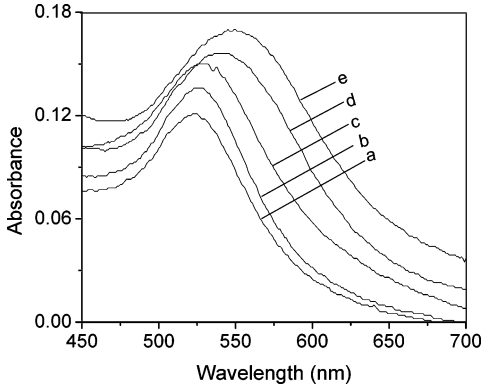

Figure 7. Absorption spectrum of gold nanoparticles (50 μM) (a) as prepared in THF and after modification with 0.1 mM of (b) C_{10}TAC, (c) C_{12}TAC, (d) C_{14}TAC, and (e) C_{16}TAC, respectively.

solvents follow a reverse trend. In their investigation, Malinsky et al.[1] observed that λ_{max} of the LSPR linearly shifts to the red by 3 nm for every carbon atom in the alkyl chain of alkanethiol adsorbates ($CH_3-(CH_2)_x-SH$) of varying chain length. Since the refractive index of all of the neat alkanethiols is roughly constant, they attributed this linear dependence on the chain length solely to an increase in the thickness of the SAM shell. The blue shift of the SAM-modified Ag particles in comparison to unmodified particles was explained in terms of alteration of the surface electronic structure of the nanoparticle donated by the S atoms of the alkanethiols.

In case of alcohols, the variation of the λ_{max} of the LSPR with the refractive index in the opposite direction clearly indicates that alcohol, being polar in character, directly interacts with gold particles by donation of the nonbonding electrons from oxygen atoms (of the −OH terminus) to the gold surfaces. Although the metal particles are stabilized through a noncovalent interaction with the surfactant moiety, the barrier to prevent the polar alcohol molecules is not sufficient enough to prevent penetrating to the surface and hence directly influences the LSPR of the metal particles. Moreover, the uniform blue shift with the increase in alcohol chain length indicates the specificity of interaction of the alcohols with the gold particles. The basic difference between binding events of the alkanethiol and alcohol is that the alkanethiols operate as the ligands, whereas alcohols act as solvents only. For alcohols with short carbon chains a large red shift of the LSPR, λ_{max}, is observed because the short molecules are more diffusing and interact more readily with the gold particles.[63] As the chain length of the alcohols increases, the diffusion of alcohol molecules to the gold particles are hindered in succession. Thus, a progressive decrease of donation of electron density onto the gold particles is understandable; therefore, a gradual blue shift is observed. The chemical interactions between the metal and its surroundings are left out of the simple dielectric environment model and so the variation in LSPR does not corroborate the variation with the refractive indices of alcohol.

3.3. Ligand Binding Effects on the LSPR of Gold Colloids. *3.3.1. Effect of Ligand Chain Length and Refractive Index.* Since naked metal nanoparticles are unstable in organic solvents, some form of stabilizer is required to prevent the particle aggregation. Encapsulation of the particle core with an appropriate shell material also offers a means of protection from the surrounding environment. These types of nanoparticles are commonly referred to as 'core−shell' particles, consisting of metal cores with a dielectric shell. Independent manipulation of the core and shell composition provides a way to engineer optical functionality. The incorporation of a shell material adds a new level of complexity to the electromagnetic modeling of the optical function due to the asymmetric environment. It is, therefore, important to understand how the interaction of the metal particles with the stabilizing ligand influences the plasma resonance. Here, we have explored the response of the LSPR with the changes in refractive index induced by the ligand binding events to the CPC-stabilized gold nanoparticles. Interestingly, it was seen that functionalized gold nanoparticles could detect changes in refractive index induced by analyte binding events.

We have selected a series of cationic (C_{10}TAC, C_{12}TAC, C_{14}TAC, and C_{16}TAC) and anionic (DSS, SDS, and SDBS) surfactants of variable chain length to detect the LSPR changes induced by the binding of these analytes to the gold colloids. It was seen that surfactants with different chain lengths induce different dielectric environments at the gold/surfactant interface and the sensitivity is reflected in the absorption spectral features of gold particles. The gold suspension in toluene was dried under vacuum and redispersed in THF (20 mL, final concentration of gold was 0.5 mM). A measured amount of C_nTAC solution (0.1 mM) in THF was introduced to the gold colloids (50 μM) and the final volume of the solution was made to 2 mL in THF. Now, the LSPR spectrum of each solution was noted after addition of the analyte to the gold colloids. Figure 7 shows the effect of addition of cationic surfactants of variable chain length on the LSRP of gold particles. As the chain length of the cationic surfactant increases, the band position gradually shifts to lower energy. In addition, the LSPR spectra increases in intensity and become broadened with an increase in chain length of the surfactant. A similar effect on the LSPR was observed with the variation in chain length of anionic surfactants (DSS, SDS, and SDBS) as shown in Figure 8. When zwitterionic amino acids were employed in lieu of surfactants, no dramatic influence on the LSPR was noticed, as illustrated in Figure 9. Malinsky et al.[1] showed that the LSPR shifts to the red by 5 nm with the adsorption of polypeptide and poly-L-lysine to Ag nanoparticles modified with deprotonated carboxylate groups from 11-mercaptoundecanoic acid. Underwood and Mulvaney[55] noted that although the use of *comb* polymers as stabilizers provides a simple pathway for the transfer of nanosized metal particles into a range of organic solvents, the surface plasmon bands are not influenced by the adsorption of epoxy groups to the metal surface.

The effect of ligand chain length on the LSPR of gold colloids can be accounted for by considering the contribution of the dielectric of the organic shell. When a metallic nanoparticle is induced by a ligand shell whose refractive index is different from that of the ambient (i.e., a gold nanocore), the field that acts on the particle is no longer homogeneous. The dense shell

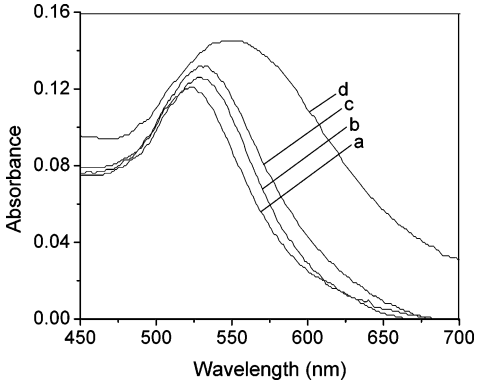

Figure 8. Absorption spectrum of gold nanoparticles (50 μM) (a) as prepared in THF and after modification with 0.1 mM of (b) DSS (c) SDS and (d) SDBS, respectively.

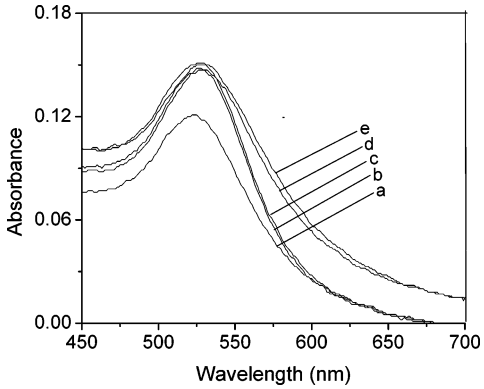

Figure 9. Absorption spectrum of gold nanoparticles (50 μM) (a) as prepared in THF and after modification with 0.1 mM of (b) glycine, (c) alanine, (d) valine, and (e) leucine, respectively.

of binding ligands provides a dielectric coating on the particle surface, amounting to a change in the dielectric constant of the medium and causing a red shift of the λ_{max} of the LSPR.[62,64,65] The gold nanocores being negatively charged (due to adsorption of negatively charged counterions), CPC^+ ions are bound to the gold surface via the headgroups and are connected to the outer layer through hydrophobic interactions.[66] Each gold particle corresponds to ca. 370 CPC molecules and each surfactant molecule amounts to ca. 0.3 nm^2 of the particle surface. When surfactants of variable chain length are introduced, the molecules are adsorbed on the surface of the gold particles by 'place exchange reaction' with the cetylpyridinium chloride[67] and interact with the gold particles with their functional groups and hydrocarbon chains. In the present experiment, as both cationic and anionic surfactants cause a red shift in the absorption spectrum, it is reasonable to assume that alteration of the refractive index is an important factor to influence the LSPR. In addition, in a system of metal particles where the combination of solvent and ligand shell are very similar in terms of refractive index, the particles may be treated as if they were in a homogeneous solvent. However, if there is a difference in the refractive index value, the field around the particles is no more homogeneous. Murray et al.[4] thus modified eq 1 by including the contribution of the dielectric of the organic shell to give a more accurate description of the surface plasmon peak position (λ) as

$$\lambda^2 = \lambda_p{}^2 [(\epsilon^\infty + 2\epsilon_m) + 2g (\epsilon_s - \epsilon_m)/3] \qquad (2)$$

The optical dielectric function of the shell layer is ϵ_s. The medium is assumed to be nonabsorbing so that ϵ_s is the dispersionless optical dielectric function of the shell and is related to the refractive index of the shell layer by the relation $\epsilon_s = n_s{}^2$. The volume fraction of the shell layer, that is, the core-to-shell volume ratio (g) is defined by

$$g = \frac{[(R_{core} + R_{shell})^3 - R_{core}{}^3]}{(R_{core} + R_{shell})^3} \qquad (3)$$

The increase in chain length of the surfactant offers a twofold influence on the LSPR of metal particles. First, according to eq 3, since g increases with an increase in chain length of the surfactant, longer-chain surfactants should shift the plasmon band position, λ, to longer wavelengths in accordance with eq 2. The increase in core-to-shell volume ratio (g) with the increase in chain length of the cationic and anionic surfactants is shown in Table 2 (considering the particle diameter as ~6 nm). Second, the refractive index of the shell layer, $n_s = \epsilon_s{}^{1/2}$, increases with the increase in surfactant chain length and, therefore, the band wavelength should increase. The increase in plasmon band intensity with the increasing thickness of the shell layer (arising due to the longer chain surfactants) is due to the attendant change in particle volume, because particle polarizability scales with particle volume. Covalent linking of the surfactants to the gold surface is likely to have some contribution in the red shifting of the LSPR, but it is not possible to isolate the contribution in the present scenario. The insignificant variation of the LSPR spectrum upon addition of amino acids of different chain length indicates nonspecific interaction of the amino acid molecules with the CPC-stabilized gold particles.

TABLE 2: Account of the Chain Length and Core-to-Shell Volume Ratio (g) of Cationic and Anionic Surfactants

cationic surfactant	chain length (nm) (R_{shell})	g	anionic surfactant	chain length (nm) (R_{shell})	g
C_{10}TAC	1.80	0.7559	DSS	1.82	0.7589
C_{12}TAC	2.08	0.7940	SDS	2.07	0.7928
C_{14}TAC	2.31	0.8197	SDBS	2.20	0.8080
C_{16}TAC	2.57	0.8438			

TABLE 3: Account of the Core-to-Shell Volume Ratio (g) and Optical Dielectric Function (ϵ_s) of Dodecylamine, Dodecanol, and Dodecanethiol

ligand	radius (nm) (R_{shell})	refractive index (n_s)	g	$\epsilon_s = n_s{}^2$
1-dodecylamine	1.77	–	0.7512	–
1-dodecanol	–	1.4572	–	2.1234
1-dodecanethiol	1.80	1.4590	0.7559	2.1287

3.3.2. Effect of Ligand Functionality. We have studied the effect of ligands containing different types of functional groups (e. g., $-NH_2$, $-OH$, and $-SH$) to see their ability to interact with gold nanoparticles. In this event, we have elegantly employed 1-dodecylamine (DDA), 1-dodecanol (DDO), and 1-dodecanethiol (DDT), which do not differ much in terms of chain length and refractive index (as shown in Table 3). When a THF solution of these ligands (0.1 mM) was introduced to the gold suspension in THF, the absorption properties of the gold particles were found to alter. Figure 10 shows the UV−vis spectra of gold nanoparticles in THF before and after addition of DDA, DDO, and DDT as shown by the traces a, b, c, and d, respectively. Figure 11 shows the dampening of LSPR of the gold colloids upon addition of a higher concentration of thiol (2 mM) as was seen due to chemisorption of I^-, SH^-, and $C_6H_5S^-$ onto the surface colloidal silver particles.[65] However, the absorption changes indicated the altered electronic state

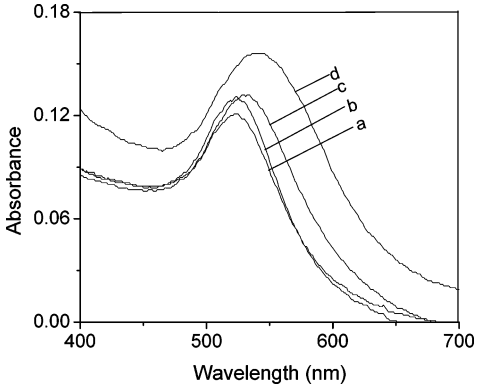

Figure 10. Optical absorption spectrum of gold nanoparticles (50 μM) (a) as prepared in THF and after modification with 0.1 mM of (b) 1-dodecylamine, (c) 1-dodecanol. and (d) 1-dodecanethiol.

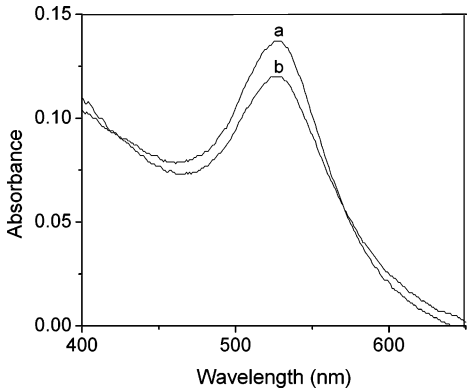

Figure 11. UV−Vis spectra of gold nanoparticles (50 μM) in THF (a) before and (b) after addition of 2.0 mM of 1-dodecanethiol.

induced by the covalent linking (i.e., chemisorption) of the gold nanocore. Since these ligands are intimately bound to the particle surface it is possible that they provide or withdraw additional electron density from the interface. The influence of such ligand binding events on the bulk metal plasmon wavelength (λ_p) of metal owing to change in the free electron density can be described by the relation

$$\lambda_p = 2\pi c/\omega_p \tag{4}$$

where c is the velocity of light in a vacuum and ω_p is the metal's bulk plasma frequency, given by

$$\omega_p = (Ne^2/m\epsilon_0)^{1/2} \tag{5}$$

where N is the free electron density and m is the electron mass.

A larger shifting (~14 nm) and broadening of the surface plasmon band were observed in the presence of DDT than were observed in the case of DDA or DDO. Moreover, we observed that the addition of DDA to DDT-modified gold particles could not bring out reasonable changes in the LSPR of the metal particles (Figure 12A). Interestingly enough, when we successively added DDT to DDA-modified gold particles, the absorption maximum gradually shifted to the red and finally showed the absorption maximum of DDT-modified gold particles (Figure 12B). Makarova et al.[68] observed that fluorescein isothiocyanate is adsorbed onto the surface of gold nanoparticles via the S atom rather than via the N atom. The trend of preferential gold−ligand interaction could be rationalized by invoking the HSAB theory. This suggests that a soft acid prefers to bind with a softer base with stronger affinity rather than a hard base.[69] Gold or any metal in the zero oxidation state has

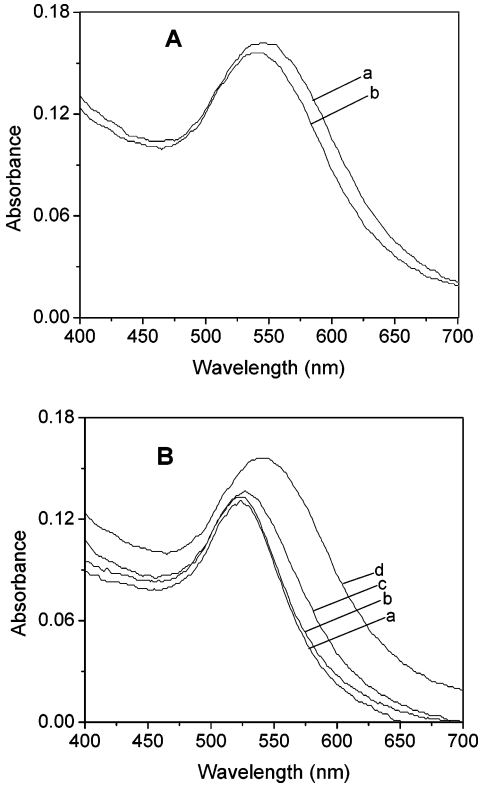

Figure 12. (A) Changes in the surface plasmon band after addition of dodecylamine (0.1 mM) (b) to dodecanethiol-modified gold nanoparticles (a) in THF. (B) Successive red shifts of the surface plasmon band upon gradual addition of (a) 0, (b) 0.02, (c) 0.05, and (d) 0.1 mM dodecanethiol to dodecylamine-modified gold nanoparticles.

TABLE 4: Atomic Radius, Polarizability and Electron Affinity of Gold, Nitrogen, Oxygen and Sulfur

elements	atomic radius (pm)	polarizability (Å^3)	electron affinity (kJ/mol)
Au	−	6.1	222.752
N	70	1.1	−6.75
O	73	0.793	140.9788
S	103	2.9	200.4144

been proven to be a softer acid than any one of their ions in the positive oxidation state. In general, softer ligands are expected to interact with the metal surface (here gold) through the lone pairs of electrons available with their headgroup/groups. The spectral shifts in the present case indicate that Au−S (soft−soft) interaction is more facile than Au−N (soft-borderline) and Au−O (soft−hard) interaction, in accordance with HSAB principle. For an overview, the atomic radii, atomic polarizability, and electron affinity of gold, nitrogen, oxygen, and sulfur are listed in Table 4. The bulk metal plasmon wavelength (λ_p) is influenced differently by the donation of variable electron density by DDA, DDO, and DDT. Consequently, the λ_{max} of the LSPR is affected. These ligands thus provide a wide range of interaction strength with the metallic particles. Ligands with amine and alcohol groups interact weakly with gold particles and preserve the electronic properties of "naked" gold surfaces. On the other hand, thiols interact strongly with the gold surface and induce significant charge redistribution.[70] In addition to electronic interaction, alkanethiols may form strong covalent bonds to the surface gold atoms through back π-bonding from the sulfur, resulting in large shifting of the LSPR predicted by simple Mie theory.

4. Conclusion

Gold nanoparticles stabilized by cetylpyridinium chloride (CPC) possess well-defined surface plasmon absorption and their formation can be investigated by following the changes in the absorption profile during the reduction process. The synthetic technique is very simple and the metal particles prepared by this method exhibit excellent solubility in nonpolar organic solvents, good air and thermal stability, a capacity to be isolated in dry form without aggregation, and an ability to be redissolved in a range of organic solvents. The metallic nanoclusters are hydrophobic in nature and stabilized by 'capping agent' with same type of functional group which is very important in view of its various applications of scientific and technological perspectives.

Solvents influence the localized surface plasmon resonance of metallic nanoclusters in two different ways. One type of solvents that does not possess any active functional group changes the refractive index at the nanoparticle/bulk interface while another group of solvents having nonbonding electrons can form complexes with the gold nanoparticle surface. Such complexation processes will override the effects of the refractive index, thereby directly affecting the LSPR of the metal colloids. The successive blue shift by ~3 nm with an increase in one carbon atom in the alcohol chain indicates the specificity of the surface complexation process with metal particles.

Introduction of the stabilizing ligand shell to the surfactant-stabilized metallic nanoclusters produces changes in the nanoparticle's local dielectric environment and in turn produces a shift in the λ_{max} of the LSPR. The shifting of the absorption maximum also depends on the core-to-shell volume ratio (g) of the metal particles and the ligand concerned. Binding studies with three model compounds that possess functional groups capable of complexing with the gold surface indicate that the fascinating interaction with the particle surface occurs in accordance with HSAB principle.

At a fundamental level, the optical absorption spectra provide information on the electronic structure of metal particles. These experimental absorption spectra can be modeled by using Mie theory for gold nanoclusters intended to mimic the influence the solvent and ligand shell in thickness and refractive index. The ligand (possessing an active functional group) binding event can be followed to see the applicability of the HSAB principle in such a microenvironment. All of this information will pave the way for the chemical synthesis of size- and shape-controlled metallic nanoclusters in organic solvents that could find a wide range of applications in chemical and biological sensors, molecular microelectronics, and other applications with highly controllable optical properties.

Acknowledgment. The authors are thankful to the Department of Science and Technology (DST) and Council of Scientific and Industrial Research (CSIR), New Delhi for financial assistance.

References and Notes

(1) Malinsky, M. D.; Kelly, K. L.; Schatz, G. C.; Van Duyne, R. P. *J. Am. Chem. Soc.* **2001**, *123*, 1471.

(2) Bain, C. D.; Evall, J.; Whitesides, G. M. *J. Am. Chem. Soc.* **1989**, *111*, 7155.

(3) Bain, C. D.; Whitesides, G. M. *J. Am. Chem. Soc.* **1989**, *111*, 7164.

(4) Templeton, A. C.; Pietron, J. J.; Murray, R. W.; Mulvaney, P. *J. Phys. Chem. B* **2000**, *104*, 564.

(5) George Thomas, K.; Zajicek, J.; Kamat, P. V. *Langmuir* **2002**, *18*, 3722.

(6) Zhang, J. Z. *Acc. Chem. Res.* **1997**, *30*, 423.

(7) Brust, M.; Walker, M.; Bethel, D.; Schiffrin, D. J.; Whyman, R. *J. Chem. Soc., Chem. Commun.* **1994**, 801.

(8) Brust, M.; Fink, J.; Bethel, D.; Schiffrin, D. J.; Kiely, C. *J. Chem. Soc., Chem. Commun.* **1995**, 1655.

(9) Vijay Sarathy, K.; Kulkarni, G. U.; Rao, C. N. R. *J. Chem. Soc., Chem. Commun.* **1997**, 537.

(10) Nakao, Y. *J. Chem. Soc., Chem. Commun.* **1994**, 2067.

(11) Lin, S. T.; Franklin, M. T.; Klabunde, K. J. *Langmuir* **1986**, *2*, 259.

(12) Esumi, K.; Kameo, A.; Suzuki, A.; Torigoe, K. *Colloids Surf., A* **2001**, *189*, 155.

(13) Porter, M. D.; Bright, T. B.; Allara, D. L.; Chidsey, C. E. D. *J. Am. Chem. Soc.* **1987**, *109*, 3559.

(14) Fendler, J. H.; Meldrum, F. C. *Adv. Mater.* **1995**, *7*, 607.

(15) Whetten, R. L.; Khoury, J. T.; Alvarez, M.; Murthy, S.; Vezmar, I.; Wang, Z. I.; Stevens, P. W.; Cleveland, C. L.; Luedtke, W. D.; Landman, U. *Adv. Mater.* **1996**, *8*, 428.

(16) Dirix, Y.; Bastiaansen, C.; Caseri, W.; Smith, P. *Adv. Mater.* **1999**, *11*, 223.

(17) Kroschwitz, J. I.; Howe-Grant, M. *Glass*, 4th ed.; Kroschwitz, J. I., Howe-Grant, M., Eds.; John Wiley & Sons: New York, 1994; Vol. 12, p 569.

(18) Krenn, J. R.; Dereux, A.; Weeber, J. C.; Bourillot, E.; Lacroute, Y.; Coadonnet, J. P. *Phys. Rev. Lett.* **1999**, *82*, 2590.

(19) Pendry, J. B. *Science* **1999**, *285*, 1687.

(20) Sanchez, E. J.; Novotny, L.; Xie, X. S. *Phys. Rev. Lett.* **1999**, *82*, 4014.

(21) Knoll, B.; Kellmann, F. *Nature* **1999**, *399*, 134.

(22) Hamann, H. F.; Gallagher, A.; Nesbitt, D. J. *Appl. Phys. Lett.* **1998**, *73*, 1469.

(23) Pufall, M. R.; Berger, A.; Schultz, S. *J. Appl. Phys.* **1997**, *81*, 5689.

(24) Wadayama, T.; Suzuki, O.; Takeuchi, K.; Seki, H.; Tanabe, T.; Suzuki, Y.; Hatta, A. *Appl. Phys. A* **1999**, *69*, 77.

(25) Tarcha, P. J.; Desaja-Gonzalez, J.; Rodriguez-Llorente, S.; Aroca, R. *Appl. Spectrosc.* **1993**, *53*, 43.

(26) Nie, S.; Emory, S. R. *Science* **1997**, *275*, 1102.

(27) Yang, W. H.; Hulteen, J. C.; Schatz, G. C.; Van Duyne, R. P. *J. Chem. Phys.* **1996**, *104*, 4313.

(28) Freeman, R. G.; Grabar, K. C.; Allison, K. J.; Bright, R. M.; Davis, J. A.; Guthrie, A. P.; Hommer, M. B.; Jackson, M. A.; Smith, P. C.; Walter, D. J.; Natan, M. J. *Science* **1995**, *267*, 1629.

(29) Pipino, A. C. R.; Schatz, G. C.; Van Duyne, R. P. *Phys. Rev. B* **1996**, *53*, 4162.

(30) Bauer, G.; Pittner, F.; Schalkhammer, T. *Mikrochim. Acta* **1999**, *131*, 107.

(31) Storhoff, J. J.; Elghanian, R.; Mucic, R. C.; Mirkin, C. A.; Letsinger, R. L. *J. Am. Chem. Soc.* **1998**, *120*, 1959.

(32) Elghanian, R.; Storhoff, J. J.; Mucic, R. C.; Letsinger, R. L.; Mirkin, C. A. *Science* **1997**, *277*, 1078.

(33) Kreibig, U.; Gartz, M.; Hilger, A. *Ber. Bunsen-Ges. Phys. Chem.* **1997**, *101*, 1593.

(34) Van Duyne, R. P.; Hulteen, J. C.; Treichel, D. A. *J. Chem. Phys.* **1993**, *99*, 2101.

(35) Malinsky, M. D.; Kelly, K. L.; Schatz, G. C.; Van Duyne, R. P. *J. Phys. Chem. B* **2001**, *105*, 2343.

(36) Kreibig, U.; Vollmer, M. *Optical Properties of Metal Clusters*; Springer: Berlin 1995.

(37) Link, S.; El-Sayed, M. A. *J. Phys. Chem. B* **1999**, *103*, 8410.

(38) Mirkin, C. A.; Ratner, M. A. *Annu. Rev. Phys. Chem.* **1997**, *101*, 1593.

(39) Rampi, M. A.; Schueller, O. J. A.; Whitesides, G. M. *Appl. Phys. Lett.* **1998**, *72*, 1781.

(40) Klein, D. L.; Roth, R.; Lim, A. K. L.; Alivisatos, A. P.; McEuen, P. L. *Nature* **1997**, *389*, 699.

(41) Bumm, L. A.; Arnold, J. J.; Cygan, M. T.; Dunbar, T. D.; Burgin, T. P.; Jones, L., II.; Allara, D. L.; Tour, J. M.; Weiss, P. S. *Science* **1996**, *271*, 1705.

(42) Ghosh, S. K.; Kundu, S.; Mandal, M.; Nath, S.; Pal, T. *J. Nanoparticle Res.* **2003**, *5*, 577.

(43) Lazarides, A. A.; Schatz, G. C. *J. Phys. Chem. B* **2000**, *104*, 460.

(44) Lazarides, A. A.; Schatz, G. C. *J. Chem. Phys.* **2000**, *112*, 2987.

(45) Pal, A.; Ghosh, S. K.; Esumi, K.; Pal, T. *Langmuir* **2004**, *20*, 575.

(46) (a) Markel, V. A.; Shalaev, V. M.; Zhang, P.; Huynh, W.; Tay, L.; Haslett, T. L.; Moskovits, M. *Phys. Rev. B* **1999**, *59*, 10903. (b) Vlckova, B.; Douketis, C.; Moskovits, M.; Shalaev, V. M.; Markel, V. A. *J. Chem. Phys.* **1999**, *110*, 8080.

(47) Faraday, M. *Philos. Trans. R. Soc. London, Ser. A* **1857**, *147*, 145.

(48) Mie. G. *Ann. Phys.* **1908**, *25*, 377.

(49) Kerker, M. *The Scattering of Light and Other Electromagnetic Radiation*; Academic Press: New York, 1969.

(50) Bohren, C. F.; Huffman, D. R. *Absorption and Scattering of Light by Small Particles*; Wiley Interscience: New York, 1983.

(51) Roy Mason, W., III.; Gray, H. B. *Inorg. Chem.* **1968**, *7*, 55.

(52) Vogel, A. I.*A Text Book of Quantitative Inorganic Analysis*, 4th ed.; Longman: London, 1978.
(53) Papavassiliou, G. C. *Prog. Solid State Chem.* **1980**, *12*, 185.
(54) Hostetler, M. J.; Wingate, J. E.; Zhong, C.-J.; Harris, J. E.; Vachet, R. W.; Clark, M. R.; Londono, J. D.; Green, S. J.; Stokes, J. J.; Wignall, G. D.; Glish, G. L.; Porter, M. D.; Evans, N. D.; Murray, R. W. *Langmuir* **1998**, *14*, 17.
(55) Underwood, S.; Mulvaney, P. *Langmuir* **1994**, *10*, 3427.
(56) Furstner, A. *Active Metals: Preparation Characterization Applications*; John Wiley & Sons: New York, 1995.
(57) Henglein, A.; Mulvaney, P.; Linnert, T. *Discuss. Faraday Soc.* **1991**, *92*, 31.
(58) Ung, T.; Giersig, M.; Dunstan, D.; Mulvaney, P. *Langmuir* **1997**, *13*, 1773.
(59) Templeton, A. C.; Wuelfing, W. P.; Murray, R. W. *Acc. Chem. Res.* **2000**, *33*, 27.
(60) Pileni, M. P. *J. Phys. Chem. B* **2001**, *105*, 3358.
(61) Henglein, A. *J. Phys. Chem.* **1993**, *97*, 5457.
(62) Mulvaney, P. *Langmuir* **1996**, *12*, 788.
(63) Pengo, P.; Pasquato, L.; Scrimin, P. *J. Supramolecular Chem.* **2002**, *2*, 305.
(64) Kelly, K. L.; Coronado, E.; Zhao, L. L.; Schatz, G. C. *J. Phys. Chem. B* **2003**, *107*, 668.
(65) Linnert, T.; Mulvaney, P.; Henglein, A. *J. Phys. Chem.* **1993**, *97*, 679.
(66) Nikoobakht, K.; El-Sayed, M. A. *Langmuir* **2001**, *17*, 6368.
(67) Boschkova, K.; Kronberg, B.; Stalgren, J. J. R.; Persson, K.; Ratoi Salagean, M. *Langmuir* **2002**, *18*, 1680.
(68) Makarova, O. V.; Ostafin, A. E.; Miyoshi, H.; Norrish, J. R., Jr.; Miesel, D. *J. Phys. Chem. B* **1999**, *103*, 9080.
(69) Huheey, J. E.; Keiter, E. A.; Keiter, R. L. *Inorganic Chemistry. Principles of Structure and Reactivity*, 4th ed.; Harper Collins: New York, 1993.
(70) Zhang, P.; Sham, T. K. *Phys. Rev. Lett.* **2003**, *90*, 245502−1.